Proceedings of the 5th International Conference on Advanced Science & Engineering ICOASE 2025, University of Zakho and Duhok Polytechnic University, 24th – 25th September 2025

(Special issue for Passer Journal of Basic and Applied Sciences)
Paper No. 16

Assessing the Accuracy of a Network of GPS Passive Stations in Duhok City

Farsat Heeto Abdulrahman [1], Sarhat M. Adam [2], Yousif Y. Zaia [2]

[1] Department of Civil Engineering, University of Zakho, Zakho 42002, Kurdistan Region, Iraq.
[2] Department of Civil Engineering, University of Duhok, Duhok 42001, Kurdistan Region, Iraq.
Email: farsat.heeto@uoz.edu.krd , sarhat@uod.ac , yousif.zaia@uod.ac

Abstract

Surveying plays a critical role in engineering projects, particularly in obtaining precise positional data for construction areas. For this purpose, accurate Reference Control Points (RCPs) are essential. RCPs can be either permanent (constructed with concrete or other materials) or temporary (used for local projects and established using GNSS positioning principles). Although temporary RCPs can be accurately determined from GNSS data through statistical analyses, their reliability tends to degrade over time. In 2011, a German company (Vossing) established a network of RCPs to support the Duhok city master plan. These RCPs have since been widely used by surveyors and engineers; however, their positional accuracy has never been systematically evaluated. This study presents the first comprehensive assessment and refinement of the Duhok RCP network using modern GNSS online processing platforms OPUS, AUSPOS, and CSRS-PPP. The RCPs were re-measured, processed, and statistically analysed to determine positional shifts and uncertainties relative to their original coordinates. Results illustrated that the mean uncertainties of approximately 27 cm in the East, 37 cm in the North, and 2.5 cm in height, corresponding to a total shift of about 46 cm with an azimuth deviation of 53° 34′ 37.709″. The findings demonstrate that long-term reliance on outdated RCP coordinates can introduce significant positional errors. This research not only quantifies the current accuracy of the Duhok network but also introduces a replicable methodology for verifying and updating control networks in regions lacking continuous GNSS reference infrastructure.

Keywords: Manuscripts; Accuracy of GCPs, Shift, Online services, analysis, Evaluation.

1 Introduction

Post-processing of static Global Navigation Satellite System (GNSS) data has become increasingly efficient through the development of numerous user-friendly, widely accessible web-based services. Prominent among these services are the Online Positioning User Service (OPUS) developed by the U.S. National Geodetic Survey (NGS), AUSPOS by Geoscience Australia, CSRS-PPP (Canadian Spatial Reference System Precise Point Positioning) offered by Natural Resources Canada, and GAPS (GNSS Analysis and Positioning Software) developed by the University of New Brunswick. These platforms have become essential tools for surveyors, engineers, and geospatial professionals, providing convenient, reliable solutions for precise positioning without the need for complex local infrastructure or advanced processing expertise [1].

Since its introduction in 2001, OPUS has gained widespread adoption in the United States for various applications, including surveying, civil engineering, geographic information systems (GIS), and mapping. Over time, OPUS has evolved to offer four solution types tailored to different observation durations and accuracy requirements, ensuring flexibility across diverse project needs [2]. Similarly, AUSPOS and CSRS-PPP have become international standards for high-precision GNSS post-processing, offering centimetre-level accuracy through advanced correction models and integration with the global reference frame [3,4,5]. These services collectively help standardize positional data and enhance spatial accuracy worldwide.

Typically, GNSS surveys involve two types of receivers: a base station, fixed at a precisely known Ground Control Point (GCP), and a rover, which collects positional data within the surveyed area. The base station coordinates are determined using the static observation method—often over 24 hours—and subsequently post-processed using licensed software such as Leica GeoOffice (LGO) or Leica Infinity [6]. Under ideal conditions, these tools provide accuracies of approximately 0.5 cm ± 1 ppm for horizontal positioning and 1 cm ± 1 ppm for vertical positioning. This high precision underscores the importance of reliable GNSS base networks as the foundation for accurate geospatial applications [7].

One of the key advantages of GNSS technology is its ability to significantly reduce the time and effort required for determining GCP coordinates. Once the GNSS receiver is positioned over the control point, data collection can be completed efficiently, and post-processing can be conducted either locally or via online platforms. However, positional accuracy can vary depending on several factors, including satellite geometry (GDOP/PDOP), ionospheric and tropospheric conditions, receiver quality, and processing strategy [8,9]. Numerous comparative studies have evaluated the performance of different post-processing methods and software packages, highlighting that the choice of processing tool can meaningfully influence positional accuracy [10,11].

Oluyori, Ono, and Okiemute (2019) [12] investigated the accuracy of several online GNSS post-processing tools, particularly focusing on height determination. Their study compared OPUS, CSRS-PPP, and Magic GNSS and concluded that these systems share similar processing methodologies and deliver highly reliable and stable coordinates. Statistical analysis using ANOVA showed no significant difference in accuracy among the evaluated services, indicating that the selection of a particular online tool often depends more on accessibility and user preference than on performance differences.

In the context of Iraq, recent research has underscored the influence of tectonic motion and seismic activity on GNSS network stability [13]. Continuous monitoring and periodic re-evaluation of control points are therefore essential to maintain the reliability of national geodetic frameworks. The city of Duhok, located in the seismically active northern region of Iraq, provides a valuable case study for such analysis. In 2011, a German surveying firm (Vossing) established 30 Ground Control Points (GCPs) across central Duhok using static GNSS methods. However, over time, these control points may have undergone coordinate shifts due to tectonic deformation, local seismic events, or environmental factors, necessitating a systematic reassessment of accuracy [14].

This study aims to evaluate the positional accuracy and consistency of a network of GPS passive stations in Duhok City using multiple online post-processing services. Specifically, GNSS observations of less than six hours will be processed through OPUS, AUSPOS, and CSRS-PPP, three well-established platforms with demonstrated reliability in international studies [9]. The research will analyse how observation duration and post-processing methodology influence coordinate accuracy and stability.

The novelty of this work lies in providing the first comprehensive accuracy assessment of Duhok's passive GNSS network, integrating modern web-based processing techniques and comparative evaluation of multiple global services. The main aim is to quantify the uncertainties in the coordinates of long-established passive GPS stations and to determine their continued suitability for geodetic, surveying, and engineering applications. The specific objectives include:

i. Collecting short-duration GNSS observations from the established GCPs

ii. Post-processing the data using OPUS, AUSPOS, and CSRS-PPP

iii. Comparing the positional accuracies derived from each service, and

iv. Identifying the optimal post-processing strategy for high-precision work in Duhok. Overall, the relevance of this study lies in improving the reliability of the local geodetic framework, supporting accurate spatial data acquisition for urban development, and contributing to the modernization of Iraq's geospatial infrastructure.

2 Related work on comparing online positioning services

Over the past decade, numerous studies have evaluated the performance of online positioning services for GNSS data processing [15]. However, many of these investigations are now outdated, as most were conducted more than 5 years ago. Consequently, they do not fully reflect recent advancements in processing algorithms, service infrastructure, or improvements in accuracy achieved through multi-GNSS integration and updated atmospheric correction models.

One of the earlier studies by Adam (2017) [16] compared online processing services such as OPUS-S, AUSPOS, and CSRS-PPP using datasets with different observation durations. The study concluded that the root mean square error (RMSE) in both horizontal and vertical components decreased with longer observation times, and that sessions of at least six hours were necessary to achieve high-accuracy results. While these findings were valuable, the research did not account for the ongoing evolution of GNSS services or evaluate their performance across diverse geographic contexts, particularly in regions with sparse infrastructure, such as northern Iraq.

Subsequent work by [17] tested five online services OPUS-S, AUSPOS, CSRS-PPP, GAPS, and Trimble RTX—using GNSS data from passive stations affected by minor to moderate multipath interference. Their results confirmed that accuracy improved with increasing observation time. However, the study did not fully account for key influencing factors such as satellite geometry (GDOP/PDOP), ionospheric and tropospheric delays, or receiver quality. These aspects are critical when evaluating service reliability in complex environments such as urban canyons or mountainous regions.

In the Iraqi context, Abdulrahman and Adam (2020) [18] examined GNSS session durations ranging from 2 to 15 hours in the Duhok region, an area with limited CORS coverage. Although their results provided valuable insight into OPUS's performance in static positioning, the study did not evaluate the effects of satellite geometry, atmospheric interference, or ambiguity resolution on accuracy. Moreover, the analysis did not incorporate the more recent improvements in GNSS processing algorithms, which have enhanced short-session performance through multi-constellation integration and refined modelling techniques.

A large-scale evaluation by Gillins et al. (2019) [2] analysed multiple versions of OPUS using 10-hour GPS datasets from 18 stations in Oregon. Their results showed that OPUS-RS consistently outperformed OPUS-S and OPUS-Net for sessions exceeding two hours, particularly in horizontal positioning and ellipsoidal height accuracy. However, their study was limited to stable environmental conditions and did not explore how factors such as receiver type, monument stability, or local atmospheric variability could affect results under different circumstances.

Earlier comparative analyses also offer a valuable perspective. Ocalan, Erdogan, and Tunalioglu (2013) [19] compared relative positioning and precise point positioning (PPP) techniques using online services including OPUS, AUSPOS, and CSRS-PPP. They found that relative positioning typically achieved sub-centimetre accuracy, while PPP methods provided accuracy around 2 cm. Nevertheless, this study did not consider ionospheric or tropospheric delays, nor did it account for multipath errors—factors that can significantly degrade accuracy, especially in dense urban or vegetated areas [20].

Overall, these earlier investigations collectively underscore that longer observation sessions generally lead to more accurate GNSS positioning. However, they often overlook dynamic factors that influence accuracy, such as satellite constellation changes, atmospheric disturbances, and receiver technology. The reliance on relative positioning techniques such as AUSPOS, which require access to nearby reference stations, also limits their applicability in remote regions where continuous reference networks are unavailable. As a result, the performance and reliability of PPP-based services such as CSRS-PPP and GAPS remain under-examined in such environments

A more recent contribution by Satchet, Wanas, and Jaber (2020) [21], titled "Estimating the Adequate Observation Times of a Single GNSS Receiver by Utilizing Online Processing Services provides a contemporary assessment of online GNSS post-processing accuracy in Iraq. The study emphasized the influence of receiver quality, observation time, and satellite geometry on positional reliability and presented comparative results for OPUS and CSRS-PPP. Their findings confirmed that both services deliver high-quality positions when appropriate observation durations and receiver configurations are used.

Additionally, several technical factors continue to play a decisive role in determining GNSS accuracy. Satellite geometry, quantified by Geometric Dilution of Precision (GDOP) and Position Dilution of Precision (PDOP) values, directly affects positional reliability, and high GDOP/PDOP values in regions with poor satellite visibility can lead to significant coordinate errors [22]. Atmospheric conditions, particularly ionospheric and tropospheric delays, also contribute to positional uncertainty, as do receiver characteristics such as signal-tracking capability, constellation support (GPS, GLONASS, Galileo, BeiDou), and ambiguity-resolution algorithms. Despite their importance, most existing studies have not comprehensively examined their combined impact on GNSS post-processing results [23,24].

Furthermore, the type of GNSS receiver and its ability to handle different satellite constellations (e.g., GPS, GLONASS, Galileo) and to resolve carrier-phase ambiguities are critical to improving accuracy, especially in challenging environments [24]. Despite these important considerations, most studies have failed to comprehensively address the full range of factors that influence GNSS performance.

In summary, previous research provides valuable insight into the general performance of online GNSS positioning services but leaves several questions unresolved. There remains a need for updated, region-specific analyses that account for technological advancements and environmental variability. The present study addresses this gap by re-evaluating the accuracy and reliability of multiple online GNSS services, OPUS, AUSPOS, and CSRS-PPP, using recent data collected from passive stations in Duhok City, Iraq, where local conditions and tectonic influences present distinct challenges to precise GNSS positioning.

3 Factors affecting the accuracy of relative positioning

3. 1 The distance error between the CORS base and the unknown point.

It is one of the main errors that occur throughout the work process. This error is unavoidable due to 2 leading causes: 1. There are no CORS stations in Duhok city, so the dependent CORS stations were ZAXO CORS base, 50 km away from the required points. 2. The electricity situation could be more stable, which would cause problems with collecting data for specific points. The websites selected to process the data automatically set the nearest CORS base with healthy data, and the data were collected when a CORS base was usually working without errors and covered the surveyed GCP session time.

3. 2 Observation time

The time of data collection is also an important factor, since it directly affects the accuracy of the sought point. The minimum time required is 2 hours, regardless of other factors. In this study, a session duration of 6 hours was aimed, which, according to an OPUS website, has an accuracy of about 1 cm for the Horizontal and vertical coordinates [25]. **Figure 1** shows that the accuracy is 2 cm ± 1 ppm for the horizontal coordinate and 2.5 cm ± 1 ppm for the vertical coordinate (ellipsoid height) (source). This OPUS accuracy is excellent for updating the old coordinates.

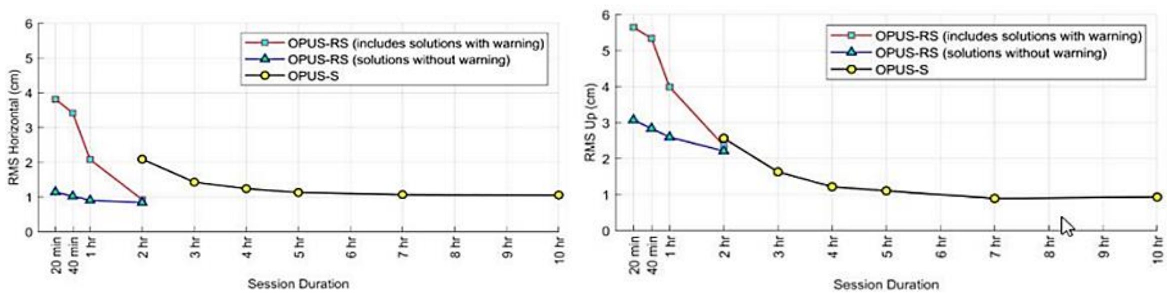

Figure 1: Theoretical accuracy of Rapid static and static modes.

3. 3 The multipath error

Like any other electromagnetic wave, GPS satellite broadcasting signals are subjected to reflection and diffraction. Multipath error results from an interaction between two radio waves that have followed different paths of different lengths between the transmitter and the receiver. The reception of signals causes GPS multipath to arrive directly from satellites and to be reflected or diffracted by local objects and atmospheric delays. Multipath errors in pseudo-range measurements (the direct distance measurement from the satellite to the GNSS receiver) degrade positioning accuracy. Since the multipath signal takes a longer path than the direct signal, this error can be reduced by placing the GCPs on a high hill and setting a cut-off angle for the satellite's signals. This surveying method is based on continuous measurements from both the base and remote receiver stations over a period, which, after processing, yield the coordinates of the unknown point. This type of survey is primarily used to create control where none exists with very high accuracy. The expected accuracy is typically 0.5 cm ± 1 ppm for horizontal coordinates and 1 cm ± 1 ppm for vertical coordinates [26,27,28].

4 Methodology and Data Collection

4. 1 Site reconnaissance and point selection

The first step in the survey process involved site reconnaissance to identify and verify the Ground Control Points (GCPs) initially established by Vossing. This verification was crucial, as the study spans multiple locations, and many monuments had been removed or damaged over time due to construction activities. For instance, two points—FP-06 and FP-21—were vandalized and removed during local construction projects (FP-06 during road construction near the K.R.O. region and FP-21 during a village construction near the French Village). However, several other points (FP-03, FP-05, FP-07, FP-08, FP-16, FP-18, FP-19, FP-20, and FP-23) were intact and were resurveyed using a GNSS device. These points, found using their original coordinates, served as the foundation for the GNSS survey as depicted in **Figure 2**.

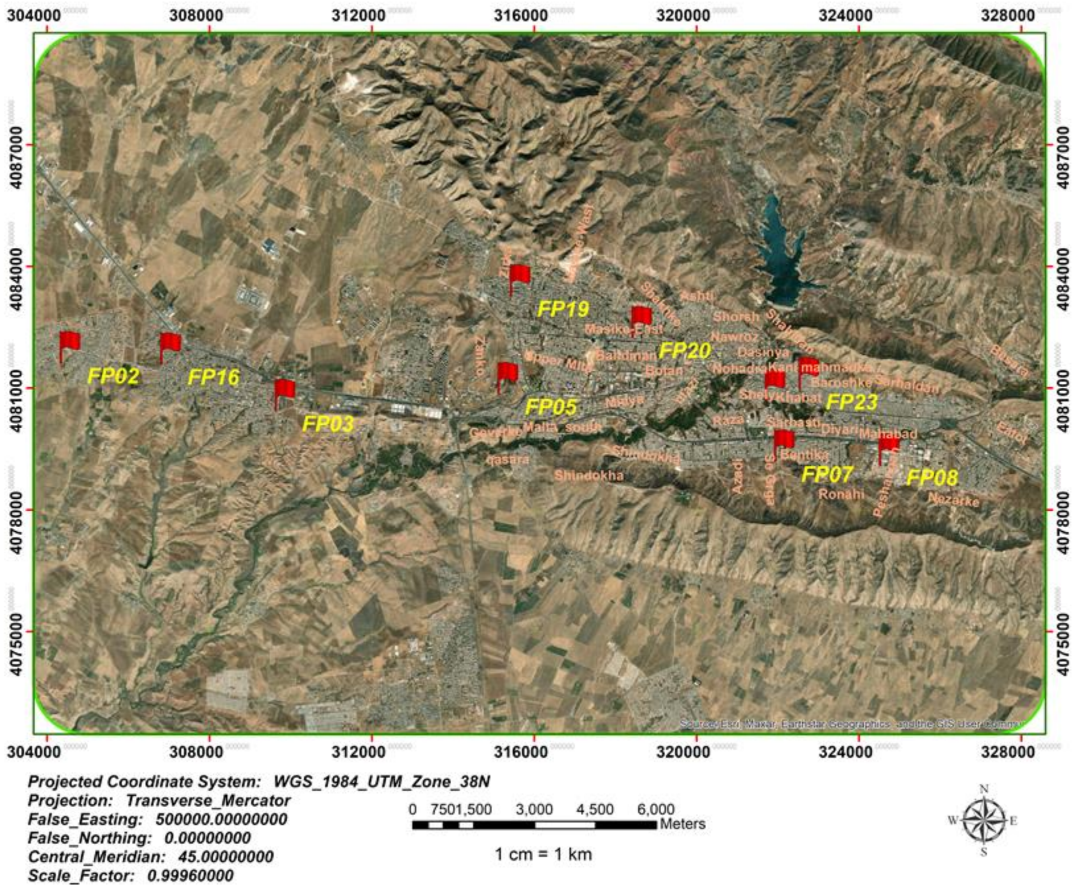

Figure 2: Map showing the distribution of available points.

4. 2 Data acquisition

Note: The GNSS data originally collected in 2019 may no longer be applicable due to potential coordinate shifts caused by tectonic motion, earthquakes, and other geophysical factors. As such, it is recommended that the data collection be updated to ensure that the results reflect the current geographical conditions. The original data, however, were processed using various online GNSS post-processing tools, and if necessary, their limitations due to geophysical changes will be addressed in future studies.

The data collection was conducted using the Leica Viva GS10 GNSS receiver with an LEIAS10 antenna. The receiver was mounted on a fixed-height tripod supported by three 25-kg concrete blocks. The antenna was calibrated to a height of 1.629 meters above the GCP. Static data were collected for 6 hours at each surveyed point. The GNSS data were saved in DBX format and imported into Leica Geo Office (LGO) to convert them to RINEX format.

The processed RINEX data were uploaded to three different online GNSS post-processing services: NOAA's OPUS, AUSPOS, and CSRS-PPP. These services allow the user to upload RINEX files and receive processed coordinates. The post-processing services are:

- NOAA's OPUS (US): Users upload the RINEX file along with the antenna type (LEIAS10) and height information. After processing, the coordinates are emailed to the user. OPUS provides reliable coordinates in the ITRF2005 and ITRF2014 reference frames [25].
- AUSPOS (Australia): AUSPOS uses a combination of IGS stations and local CORS stations. This tool typically uses up to 8 CORS stations to calculate baselines, improving accuracy over OPUS. Users receive a

report with coordinates in ITRF2014 and other systems such as GDA2020 and GDA94. The report includes detailed information about the RINEX file, including antenna type, height, and observation time [29].

- CSRS-PPP (Canada): This service provides accurate positioning based on the Canadian Spatial Reference System (CSRS). Users can upload RINEX data for static or kinematic mode. After processing, users receive a ZIP folder containing an Excel file with computed locations and a detailed report. POS and SUM formats, see Figure 3. The service utilizes precise GNSS satellite ephemerides to calculate the corrected coordinates [30] as indicated in **Figure 3**.

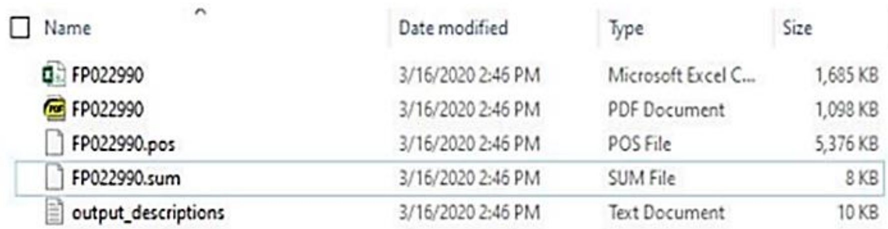

Figure 3: Content of the ZIP by CSRS-PPP.

4. 3 Static Data and Post-Processing

The static GNSS data were processed to mitigate errors like multipath, atmospheric delays, and satellite geometry issues. Each data file consisted of measurements for each epoch (1-second intervals), which were later processed using the online tools mentioned above. The post-processing output includes corrected coordinates and related metadata (e.g., satellite number, observation times, CORS stations used).

The processed coordinates received from each online service were compared for consistency and accuracy. The resulting coordinates were then used to update the GCP positions.

4. 4 Data Handling and Report Generation

After the data were processed, users received an email containing the processed coordinates, which were used to update the GCPs. The reports generated by the online tools included information such as:

- Coordinates of the surveyed point in different reference frames (e.g., ITRF, GDA2020)
- Metadata about the GNSS observations (antenna type, height, observation time, CORS stations used)
- Statistical analysis of the baselines used in the processing (for AUSPOS)
- Excel files with epoch-by-epoch positioning data (for CSRS-PPP)
- These processed results were stored for future reference and incorporated into the overall analysis of GNSS accuracy in the region.

5 Results

After the collected data are processed using the online method, the new coordinates of the GCPs and their uncertainties are tabulated in **Table 1**.

Table 1: Uncertainty values of GCPs obtained by each online service.

GCPs	Online service	Easting	Northing	Elevation	Uncertainty in Easting	Uncertainty in Northing	Uncertainty in Elevation
FP02	OPUS	304464.832	4082097.212	464.352	0.003	0.021	0.015
	AUSPOS	304464.834	4082097.208	464.354	0.009	0.008	0.024
	CSRS-PPP	304464.835	4082097.204	464.355	0.005	0.010	0.017
FP03	OPUS	309761.517	4080913.937	485.547	0.005	0.002	0.005
	AUSPOS	309761.514	4080913.937	485.534	0.007	0.006	0.020

	CSRS-PPP	309761.515	4080913.938	485.541	0.004	0.009	0.016
FP05	OPUS	315253.532	4081333.714	558.658	0.005	0.008	0.026
	AUSPOS	315253.527	4081333.714	558.630	0.008	0.006	0.021
	CSRS-PPP	315253.526	4081333.716	558.634	0.004	0.011	0.018
FP07	OPUS	322066.790	4079674.755	611.160	0.002	0.031	0.027
	AUSPOS	322066.782	4079674.747	611.170	0.011	0.009	0.035
	CSRS-PPP	322066.795	4079674.747	611.169	0.006	0.011	0.027
FP08	OPUS	324646.500	4079583.040	624.273	0.003	0.015	0.010
	AUSPOS	324646.497	4079583.039	624.273	0.008	0.007	0.020
	CSRS-PPP	324646.501	4079583.046	624.252	0.004	0.008	0.017
FP16	OPUS	306944.421	4082065.135	476.735	0.014	0.016	0.018
	AUSPOS	306944.424	4082065.113	476.777	0.012	0.009	0.037
	CSRS-PPP	306944.435	4082065.114	476.761	0.006	0.012	0.027
FP18	OPUS	321838.814	4081167.038	580.944	0.003	0.010	0.019
	AUSPOS	321838.809	4081167.044	580.946	0.007	0.006	0.021
	CSRS-PPP	321838.811	4081167.048	580.933	0.005	0.009	0.018
FP19	OPUS	31556.354	4083747.041	582.076	0.007	0.011	0.026
	AUSPOS	31556.337	4083747.043	582.049	0.009	0.008	0.023
	CSRS-PPP	31556.347	4083747.042	582.058	0.004	0.011	0.017
FP20	OPUS	318553.790	4082720.357	602.795	0.007	0.020	0.030
	AUSPOS	318553.785	4082720.352	602.808	0.009	0.008	0.026
	CSRS-PPP	318553.769	4082720.356	602.775	0.005	0.010	0.020
FP23	OPUS	322668.658	4081453.886	663.413	0.017	0.024	0.019
	AUSPOS	322668.661	4081453.874	663.413	0.010	0.008	0.027
	CSRS-PPP	322668.661	4081453.873	663.439	0.005	0.013	0.023

6 Analysis of Results and Discussion

6. 1 Statistics and calculation of the new coordinates

The online post-processed data shown in the previous section showed differences in the coordinates of each GCP across the different parameters used by the processing websites. Furthermore, the online tools can be used individually to establish new GCP coordinates. However, the results from the three online tools are combined to obtain more precise coordinates. The combined coordinate is the weighted mean coordinate obtained using equations 1-3, as shown below. The weighted mean (Easting, Northing, Elevation) is calculated using the uncertainties (sigma) of the processed data. It is important to note that the weight is inversely proportional to the sigma square. Then, the calculated coordinates can be compared with the old ones to determine the shift that has occurred during the previous years.

$$W.M.Easting = \frac{E_{OPUS}\times\frac{1}{\sigma^2_{OPUS}}+E_{AUSPOS}\times\frac{1}{\sigma^2_{AUSPOS}}+E_{CSRS-PPP}\times\frac{1}{\sigma^2_{CSRS-PPP}}}{\frac{1}{\sigma^2_{OPUS}}+\frac{1}{\sigma^2_{AUSPOS}}+\frac{1}{\sigma^2_{CSRS-PPP}}} \quad (1)$$

$$W.M.Northing = \frac{N_{OPUS}\times\frac{1}{\sigma^2_{OPUS}}+N_{AUSPOS}\times\frac{1}{\sigma^2_{AUSPOS}}+N_{CSRS-PPP}\times\frac{1}{\sigma^2_{CSRS-PPP}}}{\frac{1}{\sigma^2_{OPUS}}+\frac{1}{\sigma^2_{AUSPOS}}+\frac{1}{\sigma^2_{CSRS-PPP}}} \quad (2)$$

$$W.M.Height = \frac{H_{OPUS}\times\frac{1}{\sigma^2_{OPUS}}+H_{AUSPOS}\times\frac{1}{\sigma^2_{AUSPOS}}+H_{CSRS-PPP}\times\frac{1}{\sigma^2_{CSRS-PPP}}}{\frac{1}{\sigma^2_{OPUS}}+\frac{1}{\sigma^2_{AUSPOS}}+\frac{1}{\sigma^2_{CSRS-PPP}}} \quad (3)$$

Where W.M. (E, N, H) = Weighted Mean (Easting, Northing, Height)

(E, N, H) OPUS = (Easting, Northing, Height) from OPUS reports

(E, N, H) AUSPOS = (Easting, Northing, Height) from AUSPOS reports

(E, N, El) CSRS-PPP = (Easting, Northing, Height) from CSRS-PPP reports

σ = sigma (uncertainty of the data from the reports)

And the sigma of the weighted mean coordinates is given in the following steps:

1. Calculate the variance in equation 4

$$v = Mean\ Easting - Eastingi \quad (4)$$

2. Calculate the square variance; v 2, then

3. Calculate the sigma in equation 5

$$\sigma = \sqrt{\frac{\sum v^2}{n-1}} \quad (5)$$

After the equations above are used, a new set of weighted-mean coordinates with uncertainties is obtained. The calculated coordinates are shown in **Table 2**:

Table 2: Calculated weighted mean coordinates.

GCPs	Easting	Northing	Height	σ Easting	σ Northing	σ Height
FP02	304464.834	4082097.210	464.354	0.002	0.005	0.002
FP03	309761.515	4080913.938	485.537	0.002	0.001	0.008
FP05	315253.528	4081333.715	558.644	0.003	0.001	0.016
FP07	322066.785	4079674.754	611.167	0.008	0.007	0.006
FP08	324646.498	4079583.041	624.265	0.003	0.004	0.012
FP016	306944.423	4082065.125	476.767	0.008	0.014	0.024
FP18	321838.810	4081167.043	580.942	0.003	0.005	0.007
FP19	315556.344	4083747.042	582.063	0.009	0.001	0.014
FP20	318553.784	4082720.356	602.795	0.011	0.003	0.017
FP23	322668.659	4081453.882	663.421	0.002	0.009	0.015

6. 2 Deviation in Passive Stations

The deviation is the displacement of the Passive station points from their original location with a specific coordinate system on a specific ellipsoid or ITRF. That displacement depends on some factors. Some of them are mainly in the (Easting and Northing) shift, and some are for the elevation shift. The factors that can affect the three axes are as follows:

1. **Tectonic motion**: One of the main reasons that the coordinate of a specific point changes over the years is the tectonic motion (primarily changes in Easting and Northing of points). It is the displacement of a part of the Earth's crust in a specific direction at a specific velocity, where each part of the Earth moves in a specific direction [31] According to the references, the Arabian plate (specifically Iraq) velocity vectors moves north-eastward at about 38–40 mm per year [32], and the general motion of the Arabian Plate can be found in [33].

2. **Earthquakes:** Earthquakes occur when blocks of the Earth unexpectedly slip past one another and can cause changes in the elevation of the GCPs. This change is because, during earthquakes, the soil beneath the concrete part of the GCPs settles more such vertical deformation may alter the elevation of geodetic control points (benchmarks) anchored in these soils, as documented by geodetic monitoring studies.[34,35,36].

3. **Soil settlement:** When first installing GCP pegs, the soil beneath them should be compacted, but when the level of compaction is not entirely done, over the years, the soil tends to settle more, and so the elevation of the GCP decreases compared to the previous elevation of that point.

4. **Man-interfering factors**: When a project or any other hard work is done near the GCP place, e.g., constructing roads and buildings, these kinds of projects require heavy machines, and as they pass by the GCPs, the earth near the point may move and affect the place of the GCP and the coordinate shift by some amount.

The deviation might be due to errors in the coordinates, as the points have not been processed to obtain accurate results. The Vossing report shows that points were collected using RTK methods for 10 minutes. In addition to errors associated with RTK, the base point or the reference point might not be sufficiently accurate, leading to error propagation to the rover points.

Some of these shifts be accommodated via ITRF, for instance, tectonic motion, while others are considered to be errors in the points. In this research, WGS84 was used to compare two sets of data: the Vossing data and the data presented in this current research. Therefore, tectonic motion is not considered in this research.

Also, accidents can significantly affect the place of GCP, e.g., FP16 and FP03, as shown in **Figure 4**. FP16, as this GCP is in the middle of the road, a car accident has damaged a part of it and may have shifted its coordinates.

FP03 GCP is handled carelessly; trash is added there daily (including concrete), making the Earth heavier and affecting the GCP coordinates.

Figure 4: Ground control point, FP16 (car accident), and GCP, FP03 (trash)

The result of this study is the calculation of the shift distance and direction. The amount of shift in Easting, Northing, and Elevation individually can be calculated by subtracting new coordinates from old ones from equations 6 to 9, as shown below:

$$Shift\ in\ toward\ Easting\ (\Delta E) = Mean\ New\ Easting - Old\ Easting_i \qquad (6)$$

$$Shift\ in\ toward\ Northing\ (\Delta N) = Mean\ New\ Northing - Old\ Northing_i \qquad (7)$$

$$Shift\ in\ toward\ Heighting\ (\Delta H) = Mean\ New\ Height - Old\ Height_i \qquad (8)$$

$$3D\ distance\ error = \sqrt{(\Delta E)^2 + (\Delta N)^2 + (\Delta H)^2} \qquad (9)$$

$$Azimuth = tan^{-1}\frac{\Delta Ei}{\Delta Ni} + C \qquad (10)$$

Where C is 0 when the uncertainty lies in the first quarter, and C is 180° when the uncertainty lies in the second and third quarter, and C is 360° when the uncertainty lies in the fourth quarter

The shift of GCPs in terms of distance from the old coordinates determined by the German Vossing company in 2011is shown in **Table 3**. Directions from the true North using the equations listed above are tabulated in **Table 4** (note: positive values represent the shift toward the Easting, Northing, and rise in Height, and vice versa. The negative values represent West, South, and down in Height). The mean value is calculated by shifting the sample points to estimate the displacement for the entire network of GCPs in the central city of the Duhok region. The mean displacement shows that the network of GCPs for the central region has shifted by about 0.469 meters toward 53.577 degrees North-East. Their directions are also displayed graphically, as illustrated in **Figure 5**, **Figure 6**, and **Figure 7**.

Table 3: GCP's old coordinate by Vossing Company, 2011.

Pt. ID	Eating	Northing	Height	σ Easting	σ Northing	σ Height
FP02	304464.5748	4082096.8125	464.3918	0.0008	0.0010	0.0020
FP03	309761.2437	4080913.5637	485.5686	0.0006	0.0011	0.0017
FP05	315253.2546	4081333.3383	558.6433	0.0004	0.0003	0.0012
FP07	322066.5127	4079674.3813	611.1938	0.0004	0.0003	0.0010
FP08	324646.1926	4079582.6539	624.2781	0.0003	0.0005	0.0008
FP16	306944.1417	4082064.7494	476.8003	0.0007	0.0008	0.0025
FP18	321838.5198	4081166.6614	580.9589	0.0004	0.0003	0.0009
FP19	315556.0757	4083746.6622	582.0887	0.0004	0.0005	0.0014
FP20	318553.4874	4082719.9722	602.7904	0.0003	0.0004	0.0008
FP23	322668.3944	4081453.5390	663.4939	0.0004	0.0004	0.0010

Table 4: Calculated shifts (Distance and Direction).

Pt.ID	**Vos$_{GCP}$ - Mean$_{GCP}$**			**3D distance error (m)**	**Direction (DMS)**
	Easting	**Northing**	**Height**		
FP02	0.2593	0.3978	-0.0379	0.476303	56º54′11.666″
FP03	0.2713	0.3740	-0.0315	0.463092	54º02′22.151″
FP05	0.2734	0.3768	0.0007	0.465557	54º01′54.524″
FP07	0.2724	0.3723	-0.0268	0.462101	53º48′30.486″
FP08	0.3054	0.3871	-0.0128	0.49324	51º43′33.128″
FP16	0.2818	0.3756	-0.0337	0.47077	53º07′19.157″
FP18	0.2903	0.3813	-0.0173	0.479593	52º42′51.212″
FP19	0.2681	0.3796	-0.0257	0.465454	54º46′06.359″
FP20	0.2966	0.3841	0.0050	0.485278	52º19′17.919″
FP23	0.2645	0.3433	-0.0724	0.439414	52º23′21.438″
Mean shift	**0.2783**	**0.3772**	**-0.0252**	**0.469433**	**53º34′37.709″**

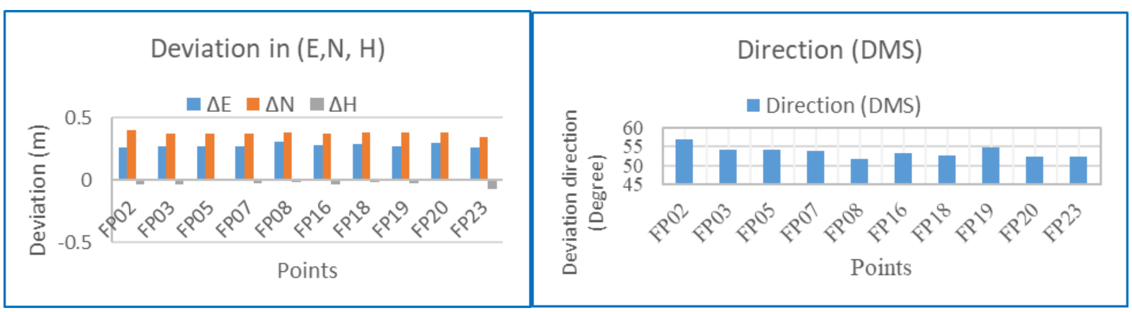

Figure 5: The position and the direction of shift.

Figure 5 (left) shows the positional deviations at several fixed points (FP02, FP03, FP05, etc.) in three components: East deviation (ΔE), the measured point differs east-west from its true position, and how far North deviation (ΔN) differs north-south; and also, for Height deviation (ΔH), the elevation differs. The ΔE and ΔN values are positive at all points, indicating that the measured coordinates are consistently shifted toward the northeast. While the values of ΔH are very small, slightly positive or slightly negative, meaning vertical measurements have much less variation compared to horizontal components. The deviations appear systematic rather than random; they do not fluctuate wildly from point to point. The magnitudes of 0.2–0.4 m horizontally and <0.1 m vertically demonstrate moderate horizontal error but small vertical error, which is typical for certain GNSS or surveying setups. This is due to possible instrumental or reference-frame bias, not to random measurement error. Figure 5 (right) also shows the direction, in degrees, of the deviation vector at each point.

The measurement system produces consistent horizontal deviations, mostly toward the northeast (≈50–55° direction). The magnitude of deviation is about 0.2–0.4 m horizontally and close to zero vertically. This pattern strongly suggests a systematic bias, not random noise, possibly caused by: GNSS satellite geometry,

reference-frame misalignment, antenna offset or calibration issue, and repeated environmental effects like multipath error.

Figure 6 shows the 3D positional error at each fixed point (FP02, FP03, FP05, etc.), indicating that the 3D error is calculated using equation 9 from the combined deviations ΔE, ΔN, and ΔH. All points show a 3D error of about 0.42-0.49 m, indicating a total positional offset of approximately half a meter. This aligns with the earlier horizontal deviations, ΔE and ΔN, of about 0.2–0.4 m, and with the very small vertical deviations. Consequently, the 3D error values are very close across all points, indicating the error is systematic rather than random, supporting the conclusion from the earlier graphs that the measurement system shifts positions in a consistent direction and magnitude. Because ΔH is very small in the previous figure, the 3D error is mainly driven by the horizontal components ΔE and ΔN. This is why the 3D values are only slightly higher than the horizontal deviations. FP08 shows the highest 3D error of about 0.49 m, meaning its horizontal deviation was slightly larger than the others. However, FP23 shows the lowest value of about 0.43 m, indicating a smaller overall deviation.

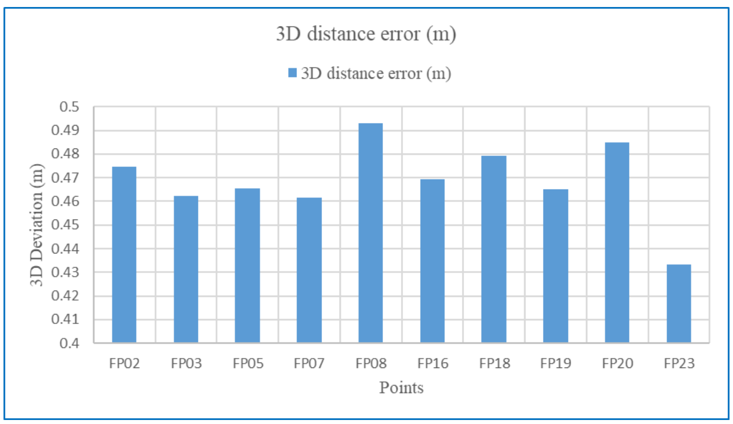

Figure 6: 3D Deviation errors

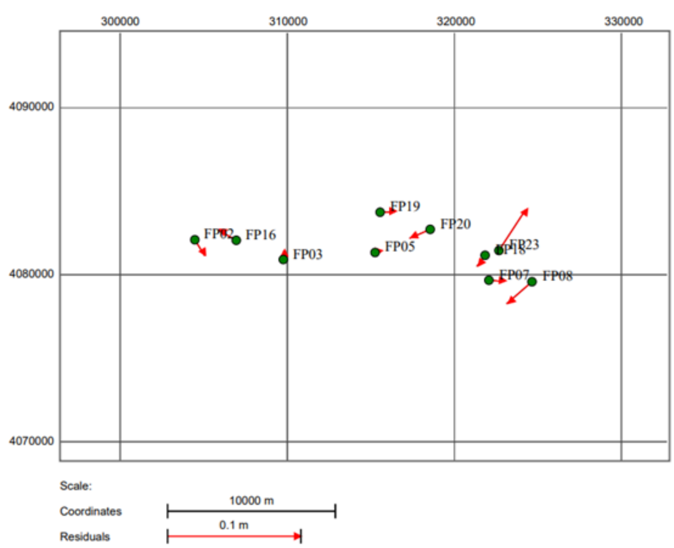

Figure 7: The position and the direction of shift between two systems of coordinates

Figure 7 illustrates the horizontal residuals between two coordinate systems for several fixed points (FP02, FP03, FP05, FP07, FP08, FP16, FP18, FP19, FP20, FP23). Each point is shown as a green dot is the reference or measured position. Red arrow: the residual vector, representing the direction and magnitude of the coordinate difference (shift) between systems. A scale bar indicates that the residual vectors represent displacements of 0.1 m, while the coordinate grid spans 10,000 m, making the residuals extremely small relative to the overall map extent. The direction of all residual arrow points is similar, generally toward the northeast (upper right) or east–northeast. This matches the patterns in earlier figures showing: $\Delta E > 0$ and $\Delta N > 0$, and the direction of residual approaches ≈ 50–55° as indicated in Figure 5 and Figure 6

Based on the ZAKHO-CORS report for OPUS, the velocity is shown in a 3D coordinate, which can be used to check the results; however, only Easting and Northing are used in the calculation, since elevation has various factors that can change in its dimension, as seen in the results before. Therefore, based on Pythagorean law, the velocity is calculated from the data given in the report as follows:

$$3D\ velocity = \sqrt{(0.0318)^2 + (0.0220)^2} = 0.03867\ m/year$$

Thus, the shift of 10 years = 0.03867*10 = 0.3867 m

7 Conclusions

This study demonstrates that Earth's surface and the WGS84 ellipsoid are dynamic, leading to temporal variations in surveyed coordinates due to tectonic activity, earthquakes, and soil settlement. Consequently, Ground Control Points (GCPs) are not fixed over time and should be re-evaluated periodically. Based on the observed shifts, it is recommended that GCPs be updated every five years using the International Terrestrial Reference Frame (ITRF).

This research shows that the 3D distance-error plot (see Figure 6) indicates a total positional deviation across all points of 0.42-0.49 m. These values result from combining the East, North, and Height deviations shown earlier. Because the vertical deviations were very small, the 3D error is dominated by horizontal error. The consistency of the 3D errors across points indicates that the measurement deviations are systematic rather than random. The map of residual vectors (see Figure 7) shows a consistent horizontal shift between the two coordinate systems. The red arrows indicate that all points are displaced in nearly the same northeast direction, with similar magnitudes of approximately 0.1–0.5 m. This uniform pattern confirms that the difference between the coordinate systems is dominated by a systematic translation rather than random measurement error or spatial distortion

The research also identified limitations in long-baseline observations, particularly at the ZAXO-CORS station, where an unreliable power supply affected signal reception and accuracy. Establishing a new, continuously powered CORS station in Duhok would significantly improve the reliability of static GNSS surveys.

Temporal variations in observation periods resulted in a mean positional shift of 0.469433 m among GCPs, underscoring the need for consistent observation schedules. The data provide valuable insight into the positional stability of control points established in 2011 and underscore the importance of extended observation time and larger datasets in future work.

These findings have practical implications for photogrammetry, surveying, and civil engineering, supporting the development of more accurate spatial reference frameworks in the Duhok region.

References

[1] Alkan, R. M., İlçi, V., Ozulu, İ. M., & Saka, M. H. A comparative study for accuracy assessment of PPP technique using GPS and GLONASS in urban areas. *Measurement, **69***, 1-8, doi: 10.1016/j.measurement.2015.03.012 (2015).

[2] Gillins, D. T., Kerr, D., & Weaver, B. Evaluation of the online positioning user service for processing static GPS surveys: OPUS-Projects, OPUS-S, OPUS-Net, and OPUS-RS. *Journal of Surveying Engineering, **145***(3), 05019002. doi: 10.1061/(ASCE)SU.1943-5428.0000280 (2019).

[3] Abd-Elazeem, M., Farah, A., & Farrag, F. Assessment study of using online (CSRS) GPS-PPP Service for mapping applications in Egypt. Journal of geodetic science, **1**(3), 233-239. doi: 10.2478/v10156-011-0001-3 (2011).

[4] El Shouny, A., & Miky, Y. Accuracy assessment of relative and precise point positioning online GPS processing services. *Journal of Applied Geodesy, **13***(3), 215-227. doi: 10.1515/jar-2018-0046 (2019).

[5] Herbert, T., & RAUFU, I. O. Comparative analysis of different online GNSS processing services. *Lagos Journal of Environmental Studies, **10***(1), 1-12. doi: https://ihafa.unilag.edu.ng/index.php/ljes/article/view/941 (2019).

[6] Geosystems, L. Leica Infinity GNSS processing and network adjustment: Technical overview. Leica Geosystems. *AG. https://leica-geosystems.com*. (2022).

[7] Correa-Muñoz, N. A., & Cerón-Calderón, L. A. Precision and accuracy of the static GNSS method for surveying networks used in Civil Engineering Precisión y exactitud del método GNSS en modo estático para redes topográficas utilizadas en ingeniería civil. *Ingeniería e Investigación, 38*. (2018).

[8] Mohammed, J., Moore, T., Hill, C., Bingley, R., & Hansen, D. An assessment of static precise point positioning using GPS only, GLONASS only, and GPS plus GLONASS. *Measurement, **88***, 121-130. doi: 10.1016/j.measurement.2016.03.048 (2016).

[9] Paziewski, J., Høeg, P., Sieradzki, R., Jin, Y., Jarmolowski, W., Hoque, M. M., . . . Lyu, H. The implications of ionospheric disturbances for precise GNSS positioning in Greenland. *Journal of Space Weather and Space Climate, **12***, 33. doi: 10.1051/swsc/20220013 (2022).

[10] Dardanelli, G., Maltese, A., Pipitone, C., Pisciotta, A., & Lo Brutto, M. NRTK, PPP or static, that is the question. Testing different positioning solutions for GNSS survey. *Remote Sensing, **13***(7), 1406. doi: 10.3390/rs13071406 (2021).

[11] Mustafin, M., Nasrullah, M., & Abboud, M. A Comparative Analysis of GNSS Processing Services for Static Measurements: Evaluating Accuracy and Stability at Different Observation Periods. *International Journal of Geoinformatics, **20***(9), 112-121. doi: 10.52939/ijg.v20i9.3553 (2024).

[12] Oluyori, P. D., Ono, M. N., & Okiemute, E. S. Modelling of Orthometric heights from Multi-Networks of GNSS/Precise Levelling in FCT, Abuja. *International Journal of Environment, Agriculture and Biotechnology (IJEAB), **4***(4), 1173-1180. doi: 10.22161/ijeab.4443 (2019).

[13] Isawi, S., Schuh, H., Männel, B., & Sakic, P. Stability analysis of the Iraqi GNSS stations. *Journal of Applied Geodesy, **16***(3), 299-312. doi: 10.1515/jag-2022-0001 (2022).

[14] Al-Taie, A. J., & Albusoda, B. S. Earthquake hazard on Iraqi soil: Halabjah earthquake as a case study. *Geodesy and Geodynamics, **10***(3), 196-204. doi: 10.1016/j.geog.2019.03.004 (2019).

[15] Ghoddousi-Fard, R., & Dare, P. Online GPS processing services: an initial study. *GPS solutions, **10***(1), 12-20. doi: 10.1007/s10291-005-0147-5 (2006).

[16] Adam, M. The Use of Online and Offline Processing Tools to Improve the Precision of a GPS Passive Station. *Journal of University of Duhok, **20***(1), 335-346. doi: 10.26682/sjuod.2017.20.1.30 (2017).

[17] Jamieson, M., & Gillins, D. T. Comparative analysis of online static GNSS postprocessing services. *Journal of Surveying Engineering, **144***(4), 05018002. doi: 10.1061/(ASCE)SU.1943-5428.0000256 (2018).

[18] Abdulrahman, F., & Adam, S. *The assessment of OPUS-Static in limited CORS area based on session duration.* Paper presented at the 6th International Engineering Conference “Sustainable Technology and Development"(IEC). (2020).

[19] Ocalan, T., Erdogan, B., & Tunalioglu, N. Analysis of web-based online services for GPS relative and precise point positioning techniques. *Boletim de ciencias geodesicas, **19***(2), 191-207. doi: 10.1590/S1982-21702013000200003 (2013).

[20] Ocalan, T. Accuracy assessment of GPS precise point Positioning (PPP) technique using different web-based online services in a forest environment. *Šumarski list, **140***(7-8), 357-367. doi: 10.31298/sl.140.7-8.4 (2016).

[21] Satchet, M. S., Wanas, S. K., & Jaber, A. S *Estimating the Adequate Observation Times of a Single GNSS Receiver by Utilizing Online Processing Services.* Paper presented at the IOP Conference Series: Materials Science and Engineering. (2020, 16-17 December 2019).

[22] Li, X., Barriot, J.-P., Lou, Y., Zhang, W., Li, P., & Shi, C. Towards millimeter-level accuracy in GNSS-based space geodesy: A review of error budget for GNSS precise point positioning. *Surveys in Geophysics, **44***(6), 1691-1780. doi: 10.1007/s10712-023-09785-w (2023).

[23] Kačmařík, M., Douša, J., Zus, F., Václavovic, P., Balidakis, K., Dick, G., & Wickert, J. *Sensitivity of GNSS tropospheric gradients to processing options.* Paper presented at the Annales Geophysicae. (2019, 18 Jun 2019).

[24] Li, B. Review of triple-frequency GNSS: ambiguity resolution, benefits and challenges. *The Journal of Global Positioning Systems, **16***(1), 1. doi: 10.1186/s41445-018-0010-y (2018).

[25] OPUS. Online Positioning User Service (OPUS). Retrieved from https://www.ngs.noaa.gov/OPUS. Retrieved April 2020, from https://www.ngs.noaa.gov/OPUS https://www.ngs.noaa.gov/OPUS (2020).

[26] Kos, T., Markezic, I., & Pokrajcic, J. *Effects of multipath reception on GPS positioning performance.* Paper presented at the Proceedings ELMAR-2010. (2010).

[27] Lau, L. *Chapter 4 - GNSS multipath errors and mitigation techniques.* (PhD GPS and GNSS Technology in Geosciences). Nottingham, University of Nottingham. Retrieved from (https://www.sciencedirect.com/science/article/pii/B9780128186176000093) (2021).

[28] Tsakiri, M., Sioulis, A., & Piniotis, G. (2017). Compliance of low-cost, single-frequency GNSS receivers to standards consistent with ISO for control surveying. *International Journal of Metrology and Quality Engineering, **8***, 11. doi: 10.1051/ijmqe/2017006

[29] AUSPOS. "AUSPOS: GNSS Data Processing Service." Geoscience Australia. Retrieved April 2020, from https://www.ga.gov.au (2020).

[30] CSRS-PPP. "Canadian Spatial Reference System - Precise Point Positioning (CSRS-PPP)." Natural Resources Canada. Retrieved April 2020, from https://www.nrcan.gc.ca. (2020).

[31] Mocnik, F.-B., & Westerholt, R. The effect of tectonic plate motion on georeferenced long-term global datasets. *International Journal of Applied Earth Observation and Geoinformation,* ***94***, 102183. doi: 10.1016/j.jag.2020.102183 (2021).

[32] Jasim, Z. N., Alhamadani, O., & Mohammed, M. U. Investigation the plate motion using operating refere. Available online at http://www.iaeme.com/ijciet/issues.asp. *International Journal of Civil Engineering,* ***9***(13), 419–429. (2018).

[33] Viltres, R., Jónsson, S., Alothman, A. O., Shaozhuo Liu, S. L., Masson, F., Doubre, C., & Reilinger, R. Present-Day Motion of the Arabian Plate. ***41***(3). doi: 10.1029/2021TC007013 (2022).

[34] Castagnetti, C., Cosentini, R. M., Lancellotta, R., & Capra, A. Geodetic monitoring and geotechnical analyses of subsidence induced settlements of historic structures. *Structural Control and Health Monitoring,* ***24***(12), e2030. doi: 10.1002/stc.2030 (2017).

[35] Doocy, S., Daniels, A., Packer, C., Dick, A., & Kirsch, T. D. The human impact of earthquakes: a historical review of events 1980-2009 and systematic literature review. *PLoS currents, 5*. doi: 10.1371/currents.dis.67bd14fe457f1db0b5433a8ee20fb833 (2013).

[36] Lyon, T., Filmer, M., & Featherstone, W. On the use of repeat leveling for the determination of vertical land motion: Artifacts, aliasing, and extrapolation errors. *Journal of geophysical research: solid earth,* ***123***(8), 7021-7039. doi: 10.1029/2018JB015705 (2018).